ON THE APPLICATION LIMIT OF THE INVISCID SMALL-PERTURBATION THEORY TO THE SECONDARY FLOW IN CASCADES

Koji MASUDA and Shintaro OTSUKA

Department of Aeronautical Engineering

(Received May 30, 1966)

ABSTRACT

The application limit of the inviscid small-perturbation theory, which was developed by Sqire, Winter[1] and Hawthorne[2], to the secondary flow in cascades is discussed by comparing the strength of trailing vortex obtained from the experiments with the one calculated by the theory.

The coincidence of the both is found to be possible at the regions in the exit main flow and at the portion adjoining main flow in the exit boundary layer. It was observed to be indispensable for getting coincidence to employ the value of vorticity (perpendicular to the flow) in the exit flow, and this fact suggests us that the boundary layer growth in cascade is a very important factor when we consider the secondary flow in cascades.

1. Introduction

When we want to solve the secondary flow in cascades by the method which was developed by Squire, Winter[1] and Hawthorne[2] and in which we regard the boundary layer as an inviscid rotational flow, we employ the small perturbation method and recognize that the results are not necessarily satisfactory for the estimation of cascade performances.

Considering the facts that we neglect the viscosity and presuppose the small velocity difference in boundary layers we can easily understand the discrepancies of results, but we have not yet arrived at the understanding how far this method will explain the phenomena of secondary flows.

The authors tried to examine the point mentioned above by comparing the semi-experimental value of the strength of trailing vortex with the theoretical one in this report.

2. Symbols

a : blade pitch
a' : pitch of blade wake perpendicular to the flow $a'=a\cos\gamma_2$
B : a half of cascade span
f : length [see Fig. 5]
n : integer
Δt : time difference [see equation (6)]
u : [see equation (B-1)]
V : velocity

V_m : mean velocity of inflow and outflow
w : component of velocity
Δw_y : [see equation (B-1)]
x, y, z: coordinates [see Fig. 1]
$\Gamma_{V\cdot A}$: actual vane (blade) circulation
γ : flow angle [see Fig. 1]
δ : boundary layer thickness
δ^* : boundary layer displacement thickness
ε : turning angle
θ : inclination angle of stream line
μ : $\mu=\delta/a'$
Ξ : [see equation (11)]
ξ, η, ζ: coordinates [see Fig. 1]
ψ : stream function
ω : vorticity
ω_1, ω_2: vorticity perpendicular to the inflow and exit flow respectively
ω_p : passage vorticity in exit flow

2.1. Subscripts

1 : upstream of cascade
2 : downstream of cascade
CL: center line of span
EX: experiment
TH: theory
T : trailing vortex
W : side wall

3. Theoretical Calculations

We use the small perturbation method in the following treatment.

Let us consider a plane perpendicular to the flow at the exit of cascade as illustrated in Fig. 1. Expressing the stream velocities which are induced in this plane by streamwise vortex (passage vorticity) as w_ξ and w_η, we get the following equation[1].

$$\frac{\partial^2\psi}{\partial\xi^2}+\frac{\partial^2\psi}{\partial\eta^2}=\omega_p \qquad (1)$$

where ω_p is the passage vorticity, and ψ is a stream function which is defined such as

$$w_\xi=\frac{\partial\psi}{\partial\eta},\quad w_\eta=-\frac{\partial\psi}{\partial\xi} \qquad (2)$$

Equation (1) is a Poisson's equation, and for convenience let us make use of the following simplification. In

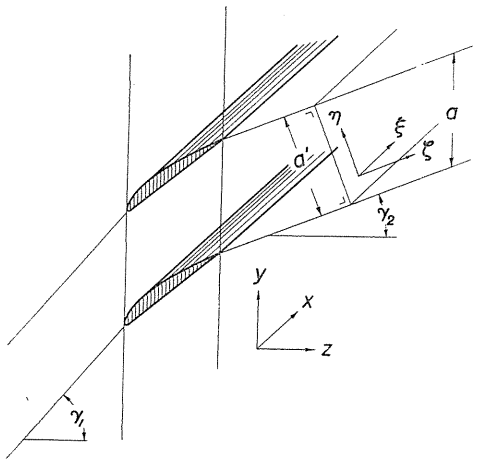

FIG. 1

the first place we assume the span of cascade to be semi-infinite. This assumption will be acceptable in the following treatment if $2B/a'$ and $2B/\delta$ (which will be referred later) are large to some extent. In the next place we assume the uniform distribution of passage vortex in the region of thickness δ adjoining the wall of cascade exit. (The calculation for the non-uniform distribution of ω_p will be treated later).

Solving equation (1) we get the induced velocities at the side wall and the blade wake as follows [from Appendix (A), (A-9)];

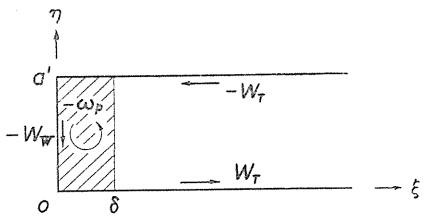

FIG. 2

$$\frac{w_W}{\omega_p\delta} = \frac{4}{\pi^2}\frac{a'}{\delta}\sum_{\substack{n=1\\ \text{odd}}}^{\infty}\frac{1}{n^2}\sin n\pi\frac{\eta}{a'}\cdot\left(1-e^{-n\pi\frac{\delta}{a'}}\right) \tag{3}$$

$$\left.\begin{aligned}\frac{w_T}{\omega_p\delta} &= -\frac{4}{\pi^2}\frac{a'}{\delta}\sum_{\substack{n=1\\ \text{odd}}}^{\infty}\frac{1}{n^2}e^{-n\pi\frac{\xi}{a'}}\left(\cosh n\pi\frac{\delta}{a'}-1\right) \qquad \delta<\xi\\ \frac{w_T}{\omega_p\delta} &= -\frac{4}{\pi^2}\frac{a'}{\delta}\sum_{\substack{n=1\\ \text{odd}}}^{\infty}\frac{1}{n^2}\left(1-e^{-n\pi\frac{\xi}{a'}}-e^{-n\pi\frac{\delta}{a'}}\sinh n\pi\frac{\xi}{a'}\right) \qquad 0\leqq\xi\leqq\delta\end{aligned}\right\} \tag{4}$$

The calculation result of w_W which is not indispensable to this study is illustrated in the Fig. 3, and the result of w_T is shown in the Fig. 4.

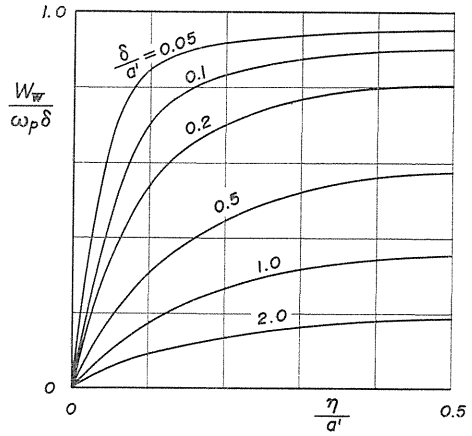

FIG. 3

4. Calculations from Experimental Values

The Fig. 5 is taken from Smith's report[3], and following this report we have

$$w_T = \frac{1}{2}\left(\omega_1 f_1 + \frac{d\Gamma_{VA}}{dx}\right) \tag{5}$$

where

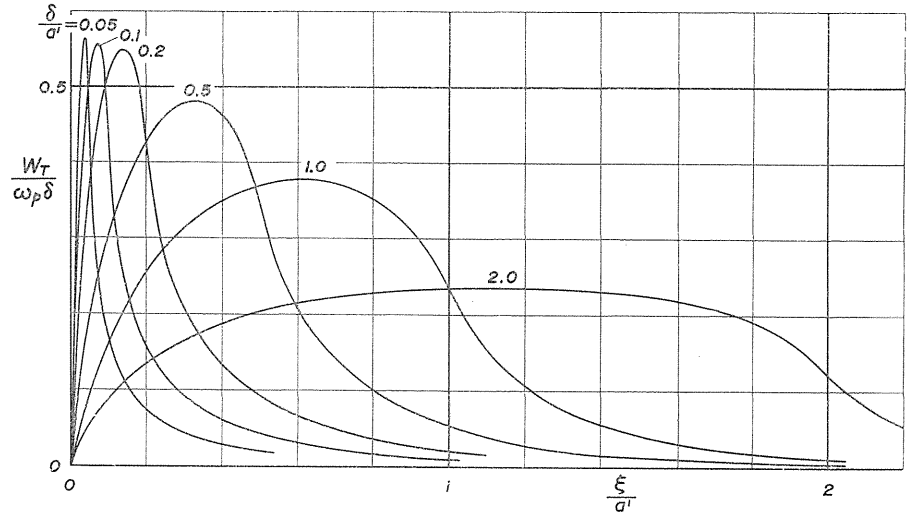

FIG. 4

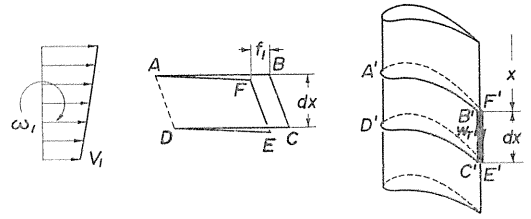

FIG. 5

$$f_1 = V_1 \Delta t$$

and Δt is the difference of times required for particles to pass lower and upper surfaces of blade, and it becomes approximately[3]

$$\Delta t = \frac{\Gamma_{V_A}}{V_m^2} \tag{6}$$

where V_m is a geometrical mean of inflow and outflow velocities. Substituting this into (5), we get

$$w_T = \frac{1}{2}\left(V_1 \omega_1 \frac{\Gamma_{V_A}}{V_m^2} + \frac{d\Gamma_{V_A}}{dx} \right) \tag{7}$$

w_T is known as the velocity at the trailing edge which forms the trailing vortex sheet, and we can find from this equation that the trailing vortex consists of two parts, one of which corresponds to the variation of blade circulation and another to the function of vortices in the inflow of cascade. And, since

$$\omega_1 = \frac{dV_1}{dx} \tag{8}$$

we get

$$w_T = \frac{1}{2}\left(V_1 \frac{dV_1}{dx} \frac{\Gamma_{VA}}{V_m^2} + \frac{d\Gamma_{VA}}{dx} \right) \tag{9}$$

Because the right side of thise quation consists of values which are obtained from actual measurements, we can get experimental value of w_T from this equation.

5. Comparison of Theoretical and Experimental Values

Let us compare values of w_T which are obtained from equations (4) and (9).

5.1. Experimental Values

Because the second term of the right side of equation (9) is the derivative of Γ_{VA} and the derivative of experimental value has much error in ordinary cases, we integrate both sides of equation (9) from ∞ (in practice, from the center of span) to x referring to the method of Hawthome and Armstrong[4]. (The integration from x to ∞ was performed in actual case to make the sign to be plus).

$$\int_x^\infty w_1 dx = \frac{1}{2}\int_x^\infty V_1 \frac{dV_1}{dx} \frac{\Gamma_{VA}}{V_m^2} dx + \frac{1}{2}[\Gamma_{VA}(x) - \Gamma_{VA}(\infty)] \tag{10}$$

After a few calculations including approximation and the non-dimensionalization [see Appendix (B)] we get

$$\Xi_{EX} = \frac{\int_x^\infty w_1 dx}{a'\int_0^\delta \omega_p dx} = \frac{1}{4(\varepsilon V_1 \cos\gamma_2)_{CL}}\left[\left(\frac{V_1 \cdot \Delta w_y}{V_m^2} \right)_{CL} \{V_{1CL} - V_1(x)\} + \{\Delta w_{yCL} - \Delta w_y(x)\} \right] \tag{11}$$

5.2. Theoretical Values

w_T which is given by equation (4) must be reformed into the type as equation (11). We can get it by the numerical integration of the Fig. 4,

$$\Xi_{TH} = \frac{\int_\xi^\infty w_T d\xi}{a'\omega_p \delta} = \int_{\xi/a'}^\infty \frac{w_T}{\omega_p \delta} d\frac{\xi}{a'} \tag{11'}$$

The results are shown in Fig. 6.

5.3. Comparison

The choice of the value of μ ($=\delta/a'$) in the Fig. 6 is important for the comparison of the experimental value and the theoretical one. In our theory we got the solution under the assumption that ω_p is constant in the boundary layer. This has the same meaning as that ω_1 is constant in the boundary layer and the distribution of V_1 must be such as the solid line in the Fig. 7. (Let us tempo rarily call this the theoretical distribution). But the actual distribution of V_1 is as illustrated by broken line in the figure. It is a problem, therefore, how to select

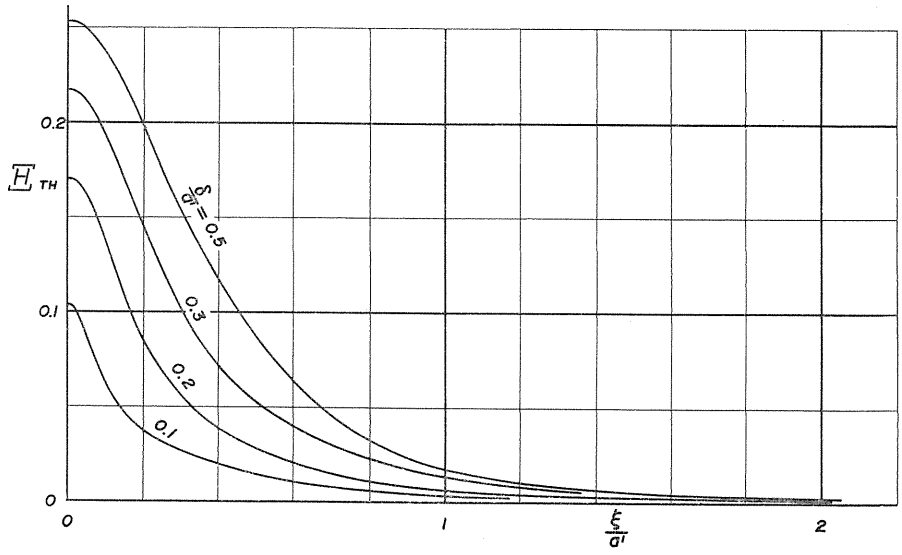

FIG. 6

the slope of solid line for the actual distribution. In other words this is the selection of the value of μ.

Figures 8～15 are the comparisons of values of Ξ calculated from the results of experiments, which were performed at the Department of Aeronautical Engineering in Nagoya University[5], and the theoretial values. Solid lines in figures are experimental values and other lines are the theoretical ones. Since there exists a problem about the selection of μ in the theoretical values as above mentioned, let us explaine it as follows;

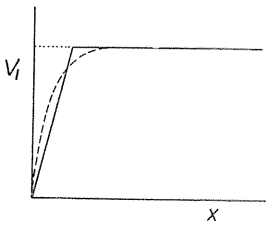

FIG. 7

a) A method in which the displacement area of boundary layer is approximated by a triangle in the theoretical distribution. Expressing the displacement thickness as δ^* we have

$$\mu = \frac{2\,\delta^*}{a'}$$

We can easily find from each figure that the theoretical values of Ξ are to osmall.

b) A method in which we use the distribution of V_2 instead of V_1. Because the boundary layer is much thicker in exit flow than inflow, we get pretty large value of μ by this method. The results are better than a) as illustrated in each figure.

c) A method in which we divide the actual velocity distribution into small straight line (constant ω_1 or ω_2) distributions. We call this method a precise treatment. There are also two ways correspond to the above cases a) and b) in which we use V_1 and V_2 respectively. In figures 8, 9, 14 and 15 we have the finely divided values of $\omega_2 = \frac{dV_2}{dx}$ and the results obtained from this ω_2 by precise

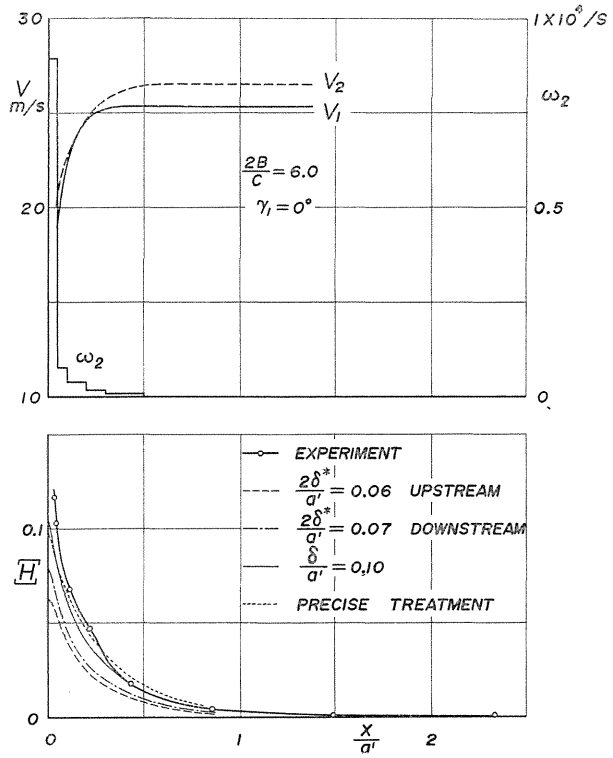
30
V
m/s
20
10
1X10⁶/S
ω2
0.5
0
V2
V1
2B/C = 6.0
γ1 = 0°
ω2
0.1
H
0
0
1
X/a'
2
EXPERIMENT
2δ*/a' = 0.06 UPSTREAM
2δ*/a' = 0.07 DOWNSTREAM
δ/a' = 0.10
PRECISE TREATMENT

FIG. 8

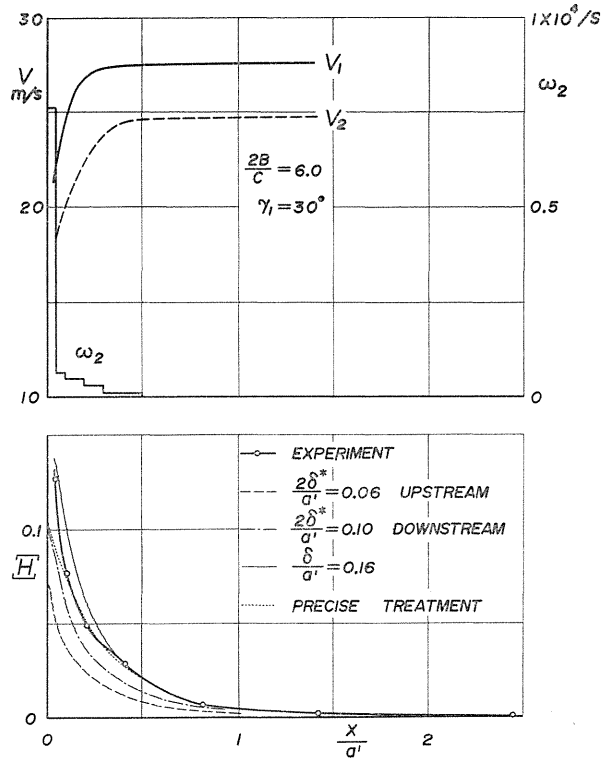
30
V
m/s
20
10
1X10⁶/S
ω2
0.5
0
V1
V2
2B/C = 6.0
γ1 = 30°
ω2
0.1
H
0
0
1
X/a'
2
EXPERIMENT
2δ*/a' = 0.06 UPSTREAM
2δ*/a' = 0.10 DOWNSTREAM
δ/a' = 0.16
PRECISE TREATMENT

FIG. 9

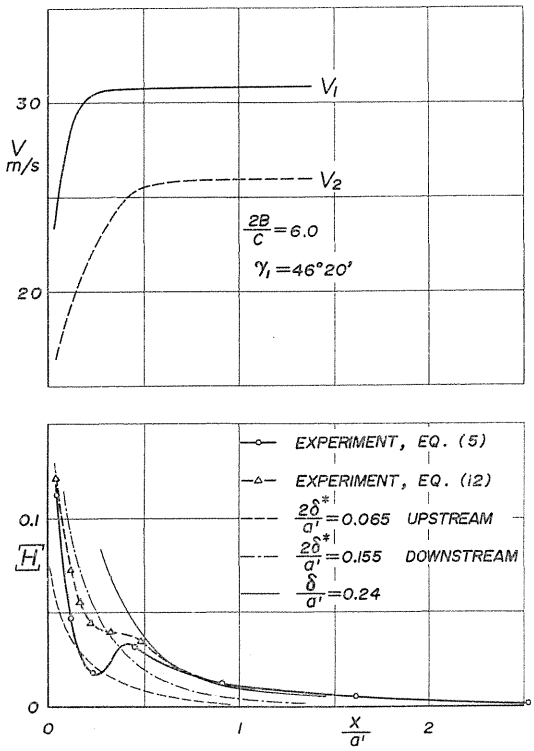
30
V
m/s
20
V_1
V_2
$\frac{2B}{C}=6.0$
$\gamma_1=46°20'$
0.1
H
0
0
1
2
$\frac{x}{a'}$
EXPERIMENT, EQ. (5)
EXPERIMENT, EQ. (12)
$\frac{2\delta^*}{a'}=0.065$ UPSTREAM
$\frac{2\delta^*}{a'}=0.155$ DOWNSTREAM
$\frac{\delta}{a'}=0.24$

FIG. 10

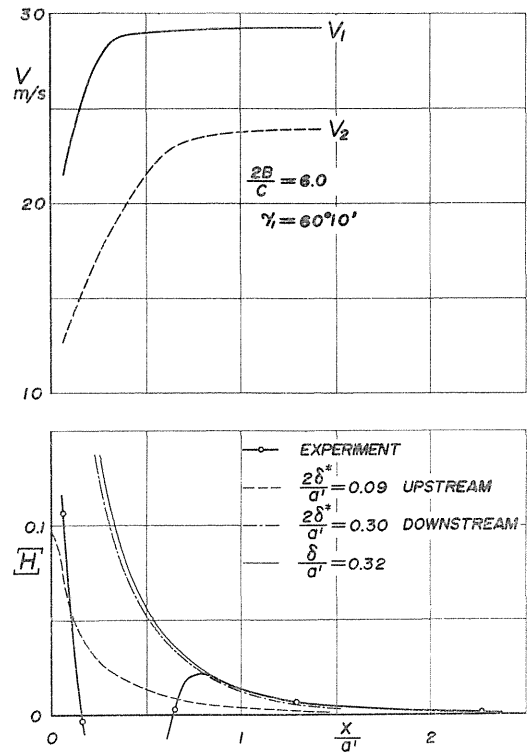
30
V
m/s
20
10
V_1
V_2
$\frac{2B}{C}=6.0$
$\gamma_1=60°10'$
0.1
H
0
0
1
2
$\frac{x}{a'}$
EXPERIMENT
$\frac{2\delta^*}{a'}=0.09$ UPSTREAM
$\frac{2\delta^*}{a'}=0.30$ DOWNSTREAM
$\frac{\delta}{a'}=0.32$

FIG. 11

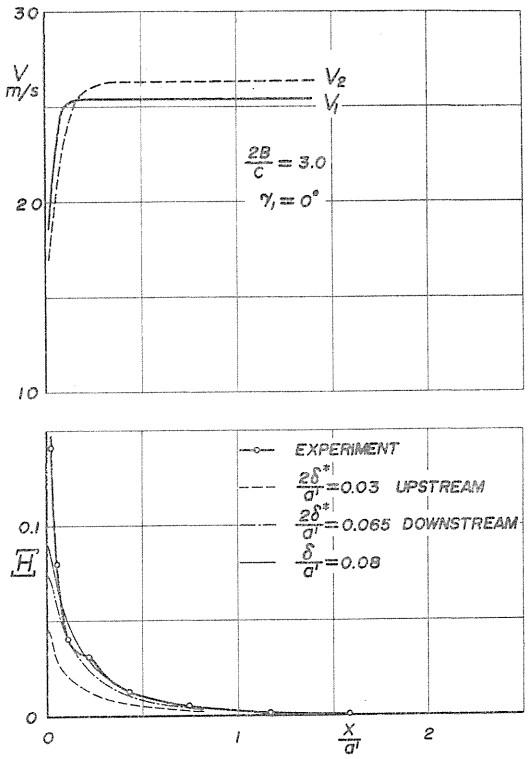
30
V
m/s
20
10
V_2
V_1
$\frac{2B}{C}=3.0$
$\gamma_1=0°$
0.1
H
0
0
1
$\frac{X}{a'}$
2
EXPERIMENT
$\frac{2\delta^*}{a'}=0.03$ UPSTREAM
$\frac{2\delta^*}{a'}=0.065$ DOWNSTREAM
$\frac{\delta}{a'}=0.08$

FIG. 12

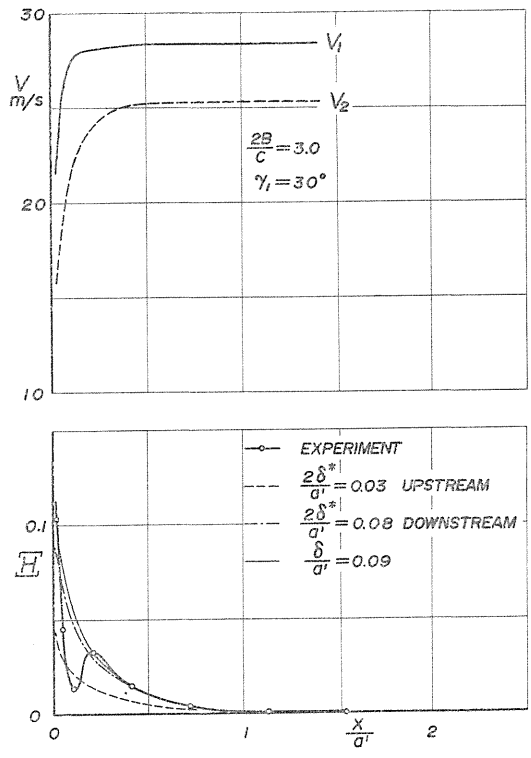
30
V
m/s
20
10
V_1
V_2
$\frac{2B}{C}=3.0$
$\gamma_1=30°$
0.1
H
0
0
1
$\frac{X}{a'}$
2
EXPERIMENT
$\frac{2\delta^*}{a'}=0.03$ UPSTREAM
$\frac{2\delta^*}{a'}=0.08$ DOWNSTREAM
$\frac{\delta}{a'}=0.09$

FIG. 13

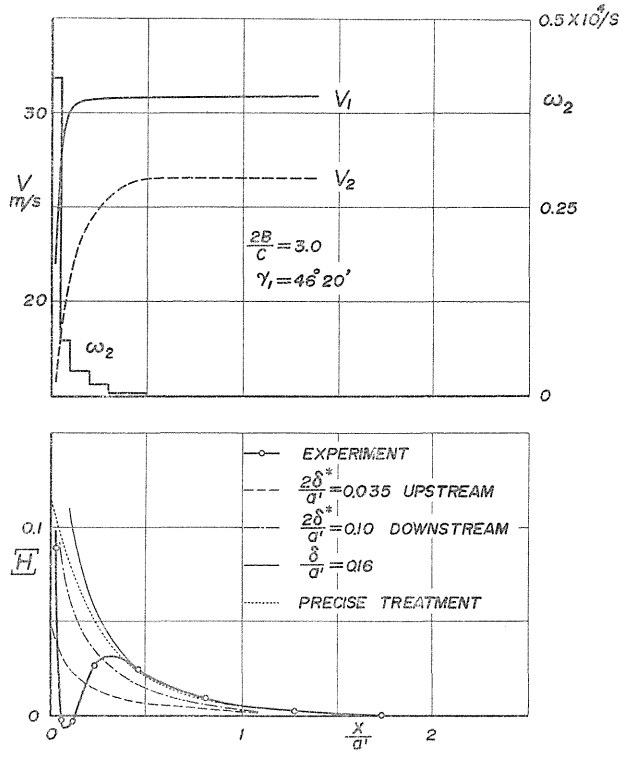
0.5X10⁴/s
30
V
m/s
20
V1
V2
ω2
0.25
0
2B/C=3.0
γ1=46°20'
ω2
EXPERIMENT
2δ*/a'=0.035 UPSTREAM
2δ*/a'=0.10 DOWNSTREAM
δ/a'=0.16
PRECISE TREATMENT
0.1
H
0
0
1
X/a'
2

FIG. 14

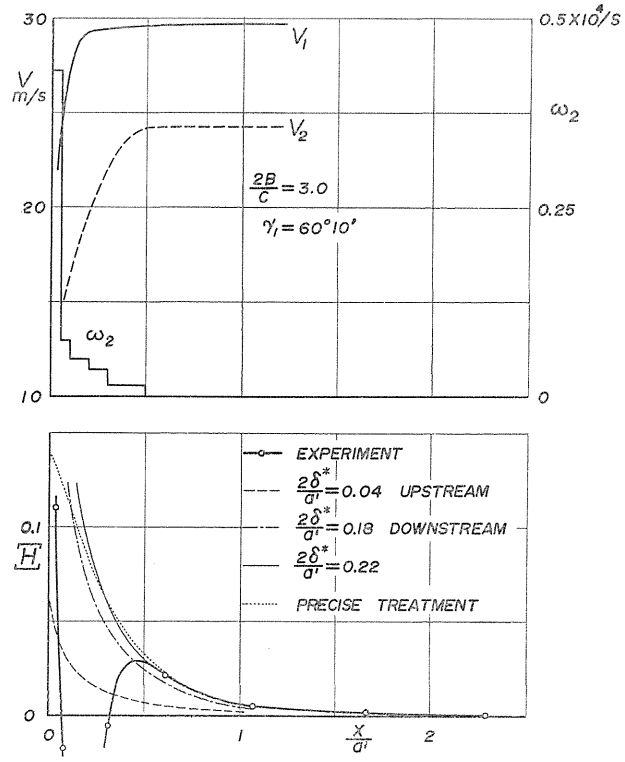
30
V
m/s
20
10
V1
V2
0.5X10⁴/s
ω2
0.25
0
2B/C=3.0
γ1=60°10'
ω2
EXPERIMENT
2δ*/a'=0.04 UPSTREAM
2δ*/a'=0.18 DOWNSTREAM
2δ*/a'=0.22
PRECISE TREATMENT
0.1
H
0
0
1
X/a'
2

FIG. 15

treatment, and we can recoginze pretty good agreement except in the region of boundary layer.

There are further shown in figures 8~15 the theoretial curves with constant ω_1 which are considered to indicate the best agreement with experimental curves. We can find from these results that the assumption of ω_1=constant has very little bad effect on the agreement provided the selection of μ is adequate.

6. Consideratons

We recognize in the above paragraph that the theoretical and experimental values can coincide in the region relatively far from the wall, *i.e.* in the main flow and in the part of boundary layer comparatively close to the main flow. But there remaines some discrepancy between the both near the wall, and this discrepancy becomes severer as the inflow angle γ_1 becomes larger. It is noteworthy that the use of V_2 curve rather than V_1 gives us better results, and this fact lead us to the idea that the boundary layer growth in cascade is a very important factor for the understanding of secondary flow phenomena. Because we took a risk to disregard this point in the derivation of equation (9), let us try to adopt another method described in the following.

In the Fig. 5 we considered a closed circut ABCDEFA which would just wrap itself around the blade, but now let us condider a closed circuit on which $\overline{BC}$ and $\overline{FE}$ overlap in the inflow such as shown in the Fig. 16. Then we have the following equation in place of equation (5).

$$w_T = \frac{1}{2}\left(\omega_2 f_2 + \frac{d\Gamma_{VA}}{dx} \right) \tag{12}$$

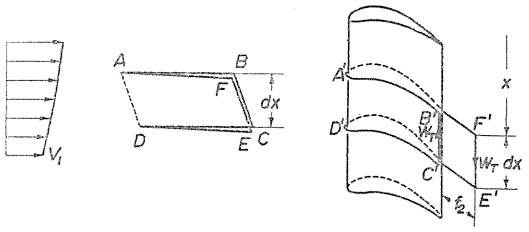

FIG. 16

Where ω_2 is vorticity perpendicular to the exit flow. Abridging the detailed treatment, one result is illustrated in Fig. 10. We recognize that far better coincidence to the theoretical value can be expected if we use the value of the exit flow.

7. Conclusion

A comparison of the strength of trailing vortices was performed to compare the theory and experiment of secondary flows in which the assumption of inviscid rotational flow and the small perturbation method were employed. A part of the theory was used to calculate the trailing vortex from the experimental results.

It was observed that the pretty good coincidence of the both is possible at

least in the main flow and in the part of boundary layer near the main flow.

We noticed that the employment of the value of the exit flow rather than inflow for the vorticity perpendicular to the flow was indispensable to the coincidence of the both, and this fact lead us to the idea that the growth of the boundary layer is a very important factor for the understanding of secondary flow phenomena in cascade.

References

1) H. B. Squire and K. G. Winter: The Secondary Flow in a Cascade of Airfoils in a Non-uniform Stream, J. Aeronautical Sciences, April 1951.
2) W. R. Hawthorne: Secondary Circulation in Fluid Flow, Proc. Royal Society of London, Ser. A. **Vol. 206**, No. A, 1086, 1951.
3) L. H. Smith: Secondary Flow in Axial-Flow Turbomachinery, Trans. ASME Oct. 1955.
4) W. R. Hawthorne and W. D. Armstrong: Rotational Flow through Cascades, Part II, The Circulation about the Cascade: Quart. J. Mechanics and Applied Mathematics, **Vol. V**, Part 3, Sept. 1955.
5) S. Otsuka and K. Masuda: An Experiment about the Effect of Aspect Ratio on Cascade Performances: Trans. Japan Society Aero. Space Sciences, **Vol. 9**, No. 14, 1966.
6) S. Otsuka: A Note about Secondary Circulation in two Dimensional Flow, J. Japan Society Aero. Sciences, Aug. 1954.

APPENDIX (A)

A 1. SOLUTION OF $\dfrac{\partial^2\psi}{\partial\xi^2}+\dfrac{\partial^2\psi}{\partial\eta^2}=\omega_p$ (1)

Determining the coordinate as illustrated in the Fig. 2, let us express ψ by the Fourier series and Fourier integral to satisfy boundary condition, *i.e.* ψ to be 0 on the boundary, such as

$$\psi(\xi,\eta)=-\sum_{n=1}^{\infty}\sin n\pi\frac{\eta}{a'}\int_0^{\infty}C_n(u)\sin u\xi du \tag{A-1}$$

Substituting this into equation (1) we get

$$\omega_p=\sum_{n=1}^{\infty}\sin n\pi\frac{\eta}{a'}\int_0^{\infty}C_n(u)\left(\frac{n^2\pi^2}{a'^2}+u^2\right)\sin u\xi du \tag{A-2}$$

From the characters of the Fourier series and integal, we have

$$C_n(u)=\frac{4}{\pi a'\left(\dfrac{n^2\pi^2}{a'^2}+u^2\right)}\int_0^{\infty}\left[\int_0^{a'}\omega_p\sin n\pi\frac{\eta'}{a'}d\eta'\right]\sin u\xi' d\xi' \tag{A-3}$$

Since ω_p is constant in regard to η, we get the integration in [ ] easily as

$$\left.\begin{aligned} C_n(u)&=\frac{8}{n\pi^2\left(\dfrac{n^2\pi^2}{a'^2}+u^2\right)}\int_0^{\infty}\omega_p\sin u\xi' d\xi' && n:\ \text{odd}\\ C_n(u)&=0 && n:\ \text{even}\end{aligned}\right\} \tag{A-4}$$

Substituting this result in (A-1) and after readjustment we have

$$\psi(\hat{\xi},\ \eta) = -\frac{8}{\pi^2}\sum_{\substack{n=1\\ \text{odd}}}^{\infty}\frac{\sin\frac{n\pi}{a'}\eta}{n}\int_0^{\infty}\frac{\sin u\hat{\xi}}{\frac{n^2\pi^2}{a'^2}+u^2}\left[\int_0^{\infty}\omega_p \sin u\hat{\xi}'d\hat{\xi}'\right]du \qquad (A\text{-}5)$$

From the assumptions,

$$\omega_p = \text{constant} \qquad 0 \leqq \hat{\xi} \leqq \delta$$
$$\omega_p = 0 \qquad \delta < \hat{\xi}$$

Therefore, we have

$$\int_0^{\infty}\omega_p \sin u\hat{\xi}'d\hat{\xi}' = \frac{\omega_p}{u}(1-\cos u\delta)$$

and

$$\int_0^{\infty}\frac{\sin u\hat{\xi}}{\frac{n^2\pi^2}{a'^2}+u^2}\left[\int_0^{\infty}\omega_p \sin u\hat{\xi}'d\hat{\xi}'\right]du$$
$$= \omega_p\int_0^{\infty}\frac{\sin n\hat{\xi}}{u\left(\frac{n^2\pi^2}{a'^2}+u^2\right)}du - \omega_p\int_0^{\infty}\frac{\sin u\hat{\xi}\cdot\cos u\delta}{u\left(\frac{n^2\pi^2}{a'^2}+u^2\right)}du$$
$$= I_1 - I_2$$

Now, let us consider I_1 and I_2 separately.

$$I_1 = \frac{\omega_p a'^2}{n^2\pi^2}\int_0^{\infty}\left(\frac{\sin u\hat{\xi}}{u} - \frac{u\sin u\hat{\xi}}{\frac{n^2\pi^2}{a'^2}+u^2}\right)du$$
$$= \frac{\omega_p a'^2}{n^2\pi^2}\left(\frac{\pi}{2} - \frac{\pi}{2}e^{-\frac{n\pi}{a'}\xi}\right)$$
$$= \frac{\omega_p a'^2}{2n^2\pi}(1-e^{-\frac{n\pi}{a'}\xi})$$

Calculation of I_2 starts from

$$\sin u\hat{\xi}\cdot\cos u\delta = \frac{1}{2}[\sin u(\hat{\xi}+\delta) + \sin u(\hat{\xi}-\delta)]$$

And using this result

$$I_2 = \frac{\omega_p a'^2}{4n^2\pi}[2 - e^{-\frac{n\pi}{a'}(\xi+\delta)} - e^{-\frac{n\pi}{a'}(\xi-\delta)}] \qquad \delta < \hat{\xi}$$
$$I_2 = \frac{\omega_p a'^2}{4n^2\pi}[e^{-\frac{n\pi}{a'}(\delta-\xi)} - e^{-\frac{n\pi}{a'}(\delta+\xi)}] \qquad 0 \leqq \hat{\xi} \leqq \delta$$

Therefore

$$\left.\begin{aligned} I_1 - I_2 &= \frac{\omega_p a'^2}{2n^2\pi} e^{-\frac{n\pi}{a'}\xi} \left(\cosh\frac{n\pi}{a'}\delta - 1\right) && \delta < \xi \\ I_1 - I_2 &= \frac{\omega_p a'^2}{2n^2\pi}\left[1 - e^{-\frac{n\pi}{a'}\xi} - e^{-\frac{n\pi}{a'}\delta}\sinh\frac{n\pi}{a'}\xi\right] && 0 \leqq \xi \leqq \delta \end{aligned}\right\}$$

Substituting these results into (A-5) we get

$$\left.\begin{aligned} \psi(\xi, \eta) &= -\frac{4\omega_p a'^2}{\pi^3}\sum_{\substack{n=1\\ \text{odd}}}^{\infty}\frac{1}{n^3}\sin\frac{n\pi}{a'}\eta \cdot e^{-\frac{n\pi}{a'}\xi}\left(\cosh\frac{n\pi}{a'}\delta - 1\right) && \delta < \xi \\ \psi(\xi, \eta) &= -\frac{4\omega_p a'^2}{\pi^3}\sum_{\substack{n=1\\ \text{odd}}}^{\infty}\frac{1}{n^3}\sin\frac{n\pi}{a'}\eta \cdot \left(1 - e^{-\frac{n\pi}{a'}\xi} - e^{-\frac{n\pi}{a'}\delta}\sinh\frac{n\pi}{a'}\xi\right) && 0 \leqq \xi \leqq \delta \end{aligned}\right\} \quad \text{(A-6)}$$

Now we have got ψ, and from equation (2) we have

$$\left.\begin{aligned} w_\xi = \frac{\partial\psi}{\partial\eta} &= -\frac{4\omega_p a'}{\pi^2}\sum_{\substack{n=1\\ \text{odd}}}^{\infty}\frac{1}{n^2}\cos\frac{n\pi}{a'}\eta \cdot e^{-\frac{n\pi}{a'}\xi}\left(\cosh\frac{n\pi}{a'}\delta - 1\right) && \delta < \xi \\ w_\xi &= -\frac{4\omega_p a'}{\pi^2}\sum_{\substack{n=1\\ \text{odd}}}^{\infty}\frac{1}{n^2}\cos\frac{n\pi}{a'}\eta \cdot \left(1 - e^{-\frac{n\pi}{a'}\xi} - e^{-\frac{n\pi}{a'}\delta}\sinh\frac{n\pi}{a'}\xi\right) && 0 \leqq \xi \leqq \delta \end{aligned}\right\} \quad \text{(A-7)}$$

$$\left.\begin{aligned} w_\eta = -\frac{\partial\psi}{\partial\xi} &= -\frac{4\omega_p a'}{\pi^2}\sum_{\substack{n=1\\ \text{odd}}}^{\infty}\frac{1}{n^2}\sin\frac{n\pi}{a'}\eta \cdot e^{-\frac{n\pi}{a'}\xi}\left(\cosh\frac{n\pi}{a'}\delta - 1\right) && \delta < \xi \\ w_\eta &= \frac{4\omega_p a'}{\pi^2}\sum_{\substack{n=1\\ \text{odd}}}^{\infty}\frac{1}{n^2}\sin\frac{n\pi}{a'}\eta \cdot \left(e^{-\frac{n\pi}{a'}\xi} - e^{-\frac{n\pi}{a'}\delta}\cosh\frac{n\pi}{a'}\xi\right) && 0 \leqq \xi \leqq \delta \end{aligned}\right\} \quad \text{(A-8)}$$

$$\left.\begin{aligned} w_W &= w_\eta(\xi = 0) \\ w_T &= w_\xi(\eta = 0) \end{aligned}\right\} \quad \text{(A-9)}$$

APPENDIX (B)

B 1. DERIVATION OF EQUATION (11)

Let us put as

$$\Gamma_{VA} = a(V_1\sin\gamma_1 - V_2\sin\gamma_2) = a \cdot \Delta w_y \quad \text{(B-1)}$$

We divide both sides of equation (10) for the non-dimensionalization by

$$a'\int_0^\delta \omega_p dx \quad \text{(B-2)}$$

Because we assumed ω_p = constant in the case of equation (4), we have

$$\int_0^\delta \omega_p dx = \omega_p\delta \quad \text{(B-3)}$$

But we consider ω_p to be a function of x in this case. Generally speaking the value of ω_p cannot be easily obtained which depends on the shape of cascade, but assuming ε to be small we can write such as [see Appendix (C)]

$$\omega_p = 2\varepsilon\omega_1 = 2\varepsilon\frac{dV_1}{dx} \tag{B-4}$$

Substituting this into (B-2)

$$a'\int_0^\delta 2\varepsilon\frac{dV_1}{dx}dx = 2a'\bar{\varepsilon}\int_0^{V_{1CL}} dV_1 = 2a'\bar{\varepsilon}V_{1CL} \tag{B-5}$$

where $\bar{\varepsilon}$ is a mean value of ε.

Using these results, let us reform equation (10),

$$\frac{\int_x^\infty w_1 dx}{a'\int_0^\delta \omega_p dx} = \frac{1}{4a'\bar{\varepsilon}V_{1CL}}\left[\int_x^\infty V_1\frac{dV_1}{dx}\frac{a\cdot\Delta w_y}{V_m^2}dx + a\{\Delta w_{yCL} - \Delta w_y(x)\}\right]$$

Because the authors recognized that $V_1\cdot\Delta w_y/V_m^2$ can be considered to be practically constant we put this out of the integral, and further we regard $\bar{\varepsilon}$ to be approximately equal to ε_{CL}, then we get the following equation from the above.

$$\frac{\int_x^\infty w_T dx}{a'\int_0^\delta \omega_p dx} = \frac{1}{4(\varepsilon V_1\cos\gamma_2)_{CL}}\left[\left(\frac{V_1\cdot\Delta w_y}{V_m^2}\right)_{CL}\{V_{1CL} - V(x)\} + \{\Delta w_{yCL} - \Delta w_y(x)\}\right] \tag{B-6}$$

APPENDIX (C)

C 1. DERIVATION OF EQUATION (B-4)

Following the first approximation theory of secondary flows[1)2)6)], we can write the passage vorticity ω_p such as the following form,

$$\omega_p = -2\omega_1\frac{V_2}{V_1}\int_{\gamma_1}^{\gamma_2}\frac{d\theta}{(V/V_1)^2} \tag{C-1}$$

where θ is the inclination angle of streamline. Therefore, we cannot get ω_p if we don't know about the flow in cascade passage. But if we assume ε to be small, we have

$$\omega_p = -2\omega_1 V_1 V_2\int_{\gamma_1}^{\gamma_2}\frac{d\theta}{\bar{V}^2}$$

$$= -2\omega_1 V_1 V_2\frac{1}{V_m'^2}(\gamma_2 - \gamma_1)$$

$$= 2\omega_1\frac{V_1 V_2}{V_m'^2}\varepsilon$$

where V'_m is a mean value between V_1 and V_2, and we may be able to put as $V'_m = \sqrt{V_1 \cdot V_2}$ under the asumption cited above. We have, therefore,

$$\omega_p = 2\,\omega_1 \varepsilon \qquad \text{(C-2)}$$